Epitaxial Crystallization and AFM Investigation of a Frustrated Polymer Structure: Isotactic Poly(propylene), β Phase

Wolfgang Stocker,*,† Martina Schumacher,‡ Sabine Graff,‡ Annette Thierry,‡ Jean-Claude Wittmann,‡ and Bernard Lotz*,‡

Institut Charles Sadron (CNRS-ULP), 6, rue Boussingault, 67083 Strasbourg, France, and Institut für Physik, Humboldt Universität zu Berlin, Invalidenstrasse 110, D-10115 Berlin, Germany

Received September 11, 1997; Revised Manuscript Received November 19, 1997

ABSTRACT: The metastable phase of isotactic polypropylene (βiPP) is crystallized epitaxially on two specific nucleating agents: γ-quinacridone and dicyclohexylterephthalamide (DCHT). The resulting thin films are investigated by electron microscopy and atomic force microscopy. Epitaxial crystallization yields a biaxially oriented sample of βiPP, an orientation which cannot be achieved by mechanical means due to the $\beta \rightarrow \alpha$ phase transformation on stretching. Electron diffraction indicates that the βiPP (110) plane is the contact face involved in both epitaxies. AFM investigation with methyl group resolution reveals a lateral periodicity of 19 Å in that (110) contact face, which corresponds to the distance between three chains and is a trademark indicator of the frustrated packing of βiPP. AFM further indicates some variability of the surface pattern, suggesting that two different frustrated structures may coexist in the surface layer; this, in turn, suggests some type of surface reconstruction. Structural requirements that efficient βiPP nucleating agents must meet are analyzed.

Introduction

The metastable β phase of isotactic poly(propylene) (βiPP) was first observed in 1959.[1] Its crystalline structure has resisted analysis for over 35 years: it was solved only in 1994.[2,3] This unusual delay, for a polymer that is known to adopt the standard three-fold helix with a 6.5 Å chain axis repeat distance also characteristic of the α and γ phases of iPP,[4,5] is due in part to the fact that βiPP cannot be obtained in fiber form: it is converted to the stable α form on stretching. As a consequence, the β phase structure has been solved mainly on the basis of *hk*0 electron diffraction patterns obtained from single crystals; part of the upper layers of the diffraction pattern was accessed by tilting the single crystals in the electron microscope stage.[2] This possibility is however limited by the available $\pm$ 60° range of tilt angles of the microscope stage.

Accessibility to the remaining part of the diffraction pattern requires that βiPP be epitaxially crystallized on adequate substrates. Being a mild orientation process, epitaxial crystallization can be used (and is actually the only means) to "fiber" orient crystal phases that, like βiPP, are mechanically unstable.[4,5] In epitaxial crystallization, the chain (or helix) axis becomes oriented parallel to the substrate surface and therefore allows observation with the electron beam *normal* to the chain axis direction (as in fiber science) rather than *parallel* to it (as in single crystals).

The unusual delay in solving the structure of βiPP is also due to its highly unconventional character in polymer science: it rests on a frustrated packing of helices.[3] Indeed, the three 3-fold isochiral helices that build up the trigonal unit cell (with $a = 11.03$ Å) have different azimuthal orientations. The helices thus have different environments, which implies that at least one of these environments is less favorable, a feature that defines frustration. The concept of frustration was introduced by Toulouse in 1977[6] to describe the conflicts created by the two mutually incompatible requirements of close packing in a hexagonal lattice and of antiparallelism of neighbor magnetic spins. Actually, the structure of isotactic poly(2-vinylpyridine) (in short iP2VP), analyzed in 1979, does have different azimuthal settings of the chains, and the resulting different helical environments have been described in much detail.[7] However, the more widespread applicability of frustration for crystal structures based on isochiral three-fold helices of chiral, and also of some achiral polymers such as iPP and iP2VP, was recognized only recently.[3,8]

Frustration in crystalline polymers and biopolymers is further complicated by the fact that two different packing schemes may be considered, which are illustrated in Figure 1. In the first, one side chain of one of the 3-fold helices is oriented (to a first approximation) north, and the side chains of the two other helices are oriented south (a scheme hereafter referred to as NSS); in the second, these side chains are oriented north east east (in short NEE) or the equivalent north west west (NWW). The former packing is observed for iP2VP[7] and was suggested as a possible model for βiPP[3] further supported by a recent reexamination of the structure.[9] The latter is closer to the structure proposed by Meille *et al.* for βiPP[2] and has also been observed in two chiral polymers: poly(*tert*-butyl ethylene sulfide) [10] and poly-(L-hydroxyproline).[11]

Investigating epitaxially crystallized βiPP is therefore of interest on several grounds: (a) it helps complete its structural investigation, by giving access to the 30° "blind cone" centered on the *c* (chain) axis which is out of reach when investigating single crystals,[9] (b) it provides a possibility to check its frustrated packing of helices and to further investigate frustration in crystalline polymers in general, and (c) in a different context, it should help establish the structural features which are at the root of βiPP nucleating agents. Nucleating agents for the β phase have been proposed and patented.

* To whom correspondence should be addressed.
† Humboldt Universität zu Berlin.
‡ Institut Charles Sadron.

S0024-9297(97)01345-4 CCC: $15.00
Published on Web 01/14/1998

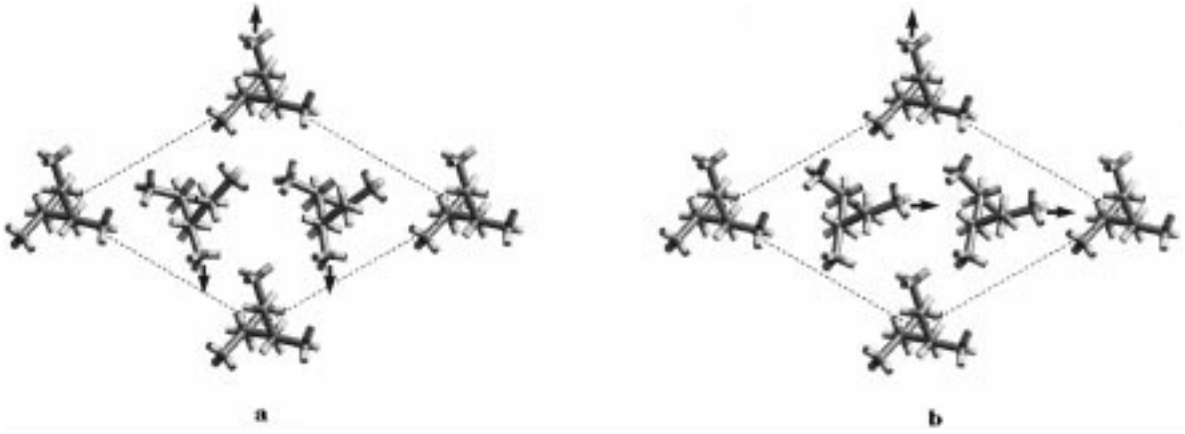

Figure 1. Crystal structure of the β phase of iPP as determined by Meille *et al.*[2] and Lotz *et al.*[3] Note the 3-fold helix geometry characteristic of all crystal polymorphs of iPP and the different azimuthal orientations of the two middle chains relative to the corner one, which creates a ≈19 Å structural periodicity in the (110) plane (horizontal). These structures can be described in short hand form by the orientation of one of their side chains (arrows) as north south south (NSS) and north east east (NEE). Helices shown are right handed; domains made of left-handed helices also exist on account of the chiral but racemic character of iPP. The statistical existence of up- and down-pointing helices (anticline helices) is not represented; such a substitution would affect only a little the position of the methyl side chains.

They make it possible to obtain virtually pure βiPP,[12−14] by enhancing the usually low "spontaneous" nucleation rate of the β phase well beyond that of the α phase, and by taking advantage of the faster growth rate of the β phase in the "conventional" crystallization range of iPP (i.e. between ≈ 140 and 105°C).[15,16]

The present paper reports on our investigation of βiPP epitaxially crystallized on different nucleating agents. Large areas of βiPP, suitable for structural investigations by electron microscopy and diffraction, and by atomic force microscopy, have been produced. The electron diffraction data are used in a parallel work dealing with a reevaluation of the crystal structure of βiPP.[9] The AFM investigations are described in the present paper. They yield the first images illustrating in real space the concept of frustration in polymer crystallography and suggest a possible surface reconstruction of epitaxially crystallized βiPP.

Experimental Section

1. Materials. The iPP samples are of various origins. Mainly two samples of high isotacticity were used, provided by ELF Aquitaine (France) and by Exxon Chemicals International (Belgium) and with molecular weights and polydispersities in the $\approx 3 \times 10^5$ range and ≈5, respectively.

Various nucleating agents were investigated, for which literature or patents indicate significant βiPP nucleating efficiency. These are as follows: γ-quinacridone, of formula $C_{20}H_{12}N_2O_2$, produced by Hoechst (Germany) under the trade name E3B[12]

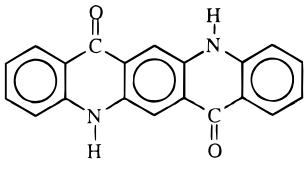

One of several thiazine derivatives examined for their βiPP nucleating effect by Garbarczyk and Paukszta,[13] namely triphenodithiazine $C_{18}H_{10}N_2S_2$ (hereafter TPDT) of structure

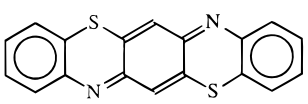

N,N′-dicyclohexylterephthalamide, $C_{20}H_{28}N_2O_2$ (hereafter DCHT), of structure

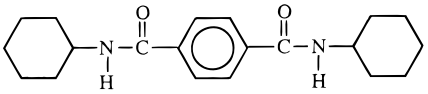

which, according to a recent patent,[14] induces the β phase of iPP with a high yield.

The crystal structures of the two former agents have been established,[17,18] but we are not aware of corresponding work for DCHT. This is most unfortunate, since the latter nucleating additive turned out to be the substrate of choice in the present investigation. Also, another patent[19] describes the βiPP nucleating action of calcium pimelate which is produced by an in-situ reaction of pimelic acid (heptanedioic acid: $HOOC(CH_2)_5COOH$) and calcium stearate. This procedure is incompatible with our experimental requirements, since relatively large (several square micrometers) substrate crystals are better suited for electron and atomic force microscopy. However, a recent patent uses the same nucleating additive, but does not rely on this in-situ reaction.[20]

2. Sample Preparation. Applying well-established techniques,[21] the epitaxial crystallization is performed by depositing crystals of the substrates on thin polymer films (20−50 nm thick) cast on glass cover slides by evaporation of a drop of a 1% solution in *p*-xylene or chlorocyclopentane. The substrate crystals are grown from semidilute (≈3 to 5%) solutions in appropriate solvents. Suitable solvents are as follows: for γ-quinacridone, dimethyl sulfoxide (DMSO) or dimethylformamide (DMF), after dissolution at 150 °C; for TPDT, DMF; for DCHT, preferrably dimethylacetamide, or a mixture of hexafluoro-2-propanol/toluene (in pure HFIP, growth of DCHT is dendritic, which is less suitable for subsequent AFM work).

After melting and recrystallization of the polymer in the crystallization range of the β phase (typically between 115 and 135 °C), the substrate crystals (which lie actually *on top* of the iPP films) are redissolved in their own solvent. The polar nature of the latter ensures that the iPP film remains unaffected in the process. The resulting thin polymer films, in which the face in contact with the nucleating agent is the exposed (top) one, are suitable for AFM work without any further processing and for electron microscopy after (optional) shadowing with Pt/C and backing with a carbon support film.

3. Techniques. Electron microscopy and diffraction are performed with a Philips CM12 instrument equipped with a 60° rotation-tilt stage. To preserve the sample from rapid damage under the electron beam, most preliminary observa-

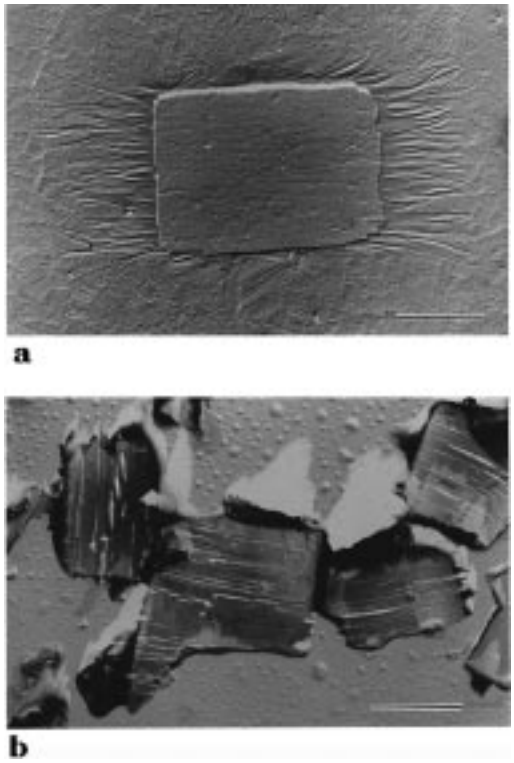

Figure 2. (a) Epitaxially crystallized thin film of βiPP on a crystal of dicyclohexylterephthalamide (DCHT). After melting and recrystallization of the iPP film, the DCHT crystal which was lying on top of the iPP film has been redissolved (but leaves its imprint) and the iPP film shadowed with Pt/C. Note the single lamellar orientation generated by the epitaxial crystallization and the further growth of βiPP lamellae in the surrounding melt. Scale bar: 5 μm. (b) Epitaxially crystallized thin film of βiPP on single crystals of γ-quinacridone. Conditions are as in part a. Scale bar: 5 μm.

tions are made at very low magnification, usually by defocussing the diffraction pattern. Bright field and diffraction patterns are recorded on Agfa Scientia EM and Kodak DEF 5 films, respectively.

Atomic force microscopy is carried out with a Nanoscope III (Digital Instruments, Inc., Santa Barbara, CA) in the contact mode. Images are obtained with an A-type scan head (maximum scan size $\approx$ 1 μm^2). Si_3N_4 tips attached to a microfabricated cantilever (triangular base, 200 μm) with a force constant of 0.06 N/m are used. With the help of an optical microscope, the tip is positioned close to the surface of preselected oriented β phase regions, which are easily recognizable due to the imprint left by the nucleating agent in the polymer film (cf. Figure 2a, b).

The high-resolution AFM images are recorded in the glass fluid cell which makes it possible to probe the polymer film while it is immersed in liquid media. The liquid cell is used as indicated by the supplier. It is limited on its lower face by the sample (on a cover slide) and on its top face by the glass of the cantilever holder and is limited laterally by an O-ring. Due to the limited elasticity of the O-ring, the lateral range of the liquid cell attachment is significantly smaller than in conventional AFM. Therefore, large scale images are first recorded without the O-ring to visualize the lamellar structure, prior to addition of the immersion liquid (2-propanol, a nonsolvent of the polymer) and high-resolution work.

Scanning line frequencies range from 1 Hz when visualizing the lamellar structure (scanned area: $\approx$ 1 μm^2) up to 54 Hz for high resolution work. In order to calibrate the distances indicated by the piezo controller, measurements on mica are performed under the same conditions: distances are usually underevaluated by about 5%. Imaging was performed by displaying the deflection signal (incoming signal for the feedback system) and the height signal (output of the feedback signal). Images presented are unfiltered deflection images.

Probing polymers in organic liquids reduces the capillary forces caused by water films on their surface. Contrary to measurements in air, the AFM force curves show less hysteresis. Therefore, images can be recorded over a wide range of separation distances between the tip and polymer surface. The high-resolution pictures could only be obtained when reducing the loading forces to values much smaller than 10^{-10} N, as determined from force curves. No band-pass filters were applied during imaging.

The quality of the tip can be checked by rotating the sample with respect to the tip. Such rotations are easy to monitor in the present case, since the epitaxially crystallized films display a single orientation of the lamellae and the chains over areas as large as $\approx$20 $\times$ 30 μm^2. Multiple tip imaging would result in different moiré patterns when rotating the sample relative to the tip; such moiré patterns were never observed. Further, several sets of experiments were performed using different tips and with various tip/sample orientations with constant and reproducible results.

Molecular modeling was performed using the Cerius^2 program developed by Biosym-Molecular Simulations (Waltham, Mass. and Cambridge, UK) run on a Silicon Graphics Indigo 2 workstation.

Results and Discussion

1. Electron Microscopy and Electron Diffraction Investigation. Out of the various substrates investigated, we were more successful with γ-quinacridone and DCHT than with TPDT: DCHT in particular is easily obtained in the form of "large" rectangular single crystals (tens of μm lateral dimensions) well suited for EM and AFM work. Parts a and b of Figure 2 represent a thin film of iPP epitaxially crystallized on crystals of DCHT and γ-quinacridone, respectively. The crystals have been redissolved but leave their imprint in the iPP film. The iPP lamellae are all parallel, suggesting a single chain orientation. Since the lamellae are seen edge-on, it is easy to estimate the lamellar thickness, which is not perfectly uniform: it ranges from $\approx$15 to 30 nm. Note also for DCHT the further growth of βiPP lamellae into the thicker film of surrounding melt, illustrating its β nucleating action (no such growth is seen in Figure 2b: the thinner polymer film used migrated by capillarity under the γ-quinacridone crystal while in the molten state).

Figure 3 represents diffraction patterns of a composite DCHT−iPP bilayer after partial (Figure 3a) and complete (Figure 3b) dissolution of the DCHT crystals, which are usually significantly thicker than the iPP film. Indexing of the pattern, generated with the Cerius 2 program, is shown in Figure 3c. Whereas the analysis of these patterns is detailed elsewhere,[9] it is worth emphasizing that, on the third layer line, the relative intensities of the 013 and 003 are fully compatible with a frustrated structure: the weakness of the meridional 003 reflection results from a *c*/6 shift of two helices in the cell, which translates into an opposition of phases with respect to 003. It lead Turner-Jones *et al.*[22] to rule out for βiPP a possible one chain unit cell with $P3_1$ or $P3_2$ symmetry. Besides confirming the frustrated structure of βiPP, the patterns indicate that a βiPP plane of (110) type is in contact with the DCHT crystal surface (zone axis [100]). Similar patterns (not shown) are obtained with γ-quinacridone and indicate that the (110) face of βiPP is also involved in that epitaxy.

The general outlines of the structural relationship between iPP and these two nucleating agents are deferred to the last section of the present discussion.

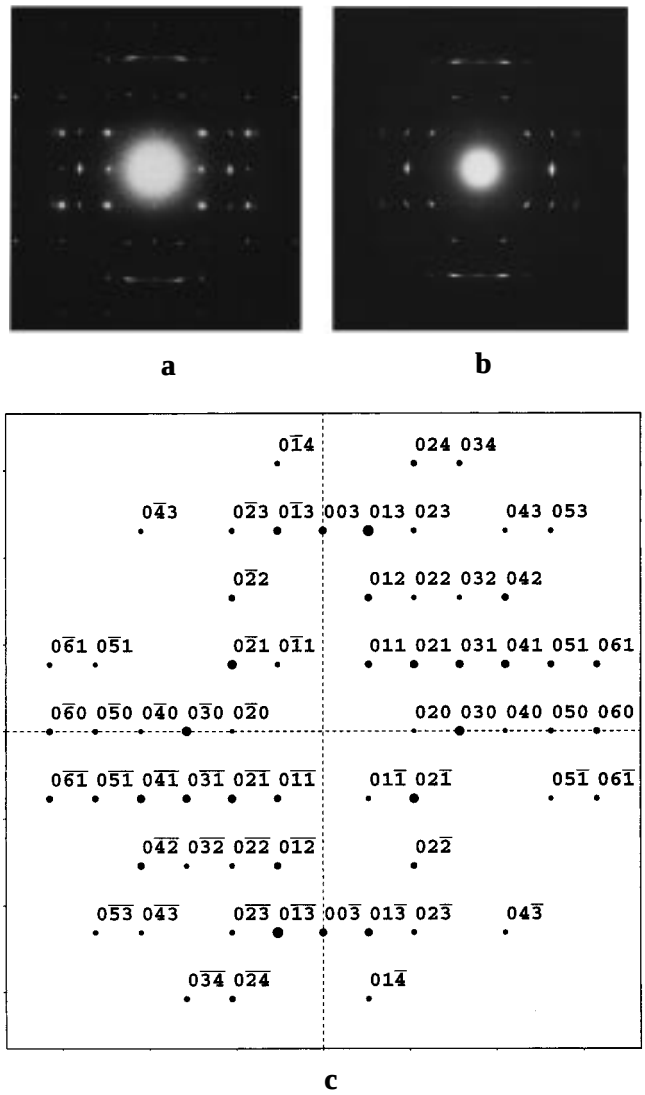

Figure 3. (a) Electron diffraction pattern of the epitaxially crystallized film shown in Figure 2a after only partial dissolution of the substrate DCHT crystal: the sharp spots correspond to DCHT and the broader ones to iPP. The chain axis is vertical. (b) Electron diffraction pattern of the epitaxially crystallized film shown in Figure 2a, i.e., after complete dissolution of the substrate DCHT crystal. (c) Model of the diffraction pattern of iPP shown in part b, using the Cerius[2] program of Molecular Simulations. Zone axis: [100]. Note the asymmetry of the pattern relative to the *c** axis, since helices of one hand only are considered in the modelization. *A contrario*, the symmetry of the actual pattern displayed in part b indicates that a nearly equal number of antichiral domains and/or lamellae coexist in the epitaxial film shown in Figure 2.

From examination of Figure 3a, we note already that the cell projection of DCHT has a strong 6.5 Å periodicity which matches the *c* axis layer line of βiPP ($\approx$ 6.5 Å). A similar matching exists for the "turn" layer line of βiPP and a strong layer line of γ-quinacridone, the structure of which has been established recently.[17]

Whereas electron diffraction indicates that the dense (110) contact plane of βiPP is involved in the epitaxy, it does not provide a complete picture of the polymer/substrate relationship. Indeed, given the various possible frustrated structures, it remains to establish, (a) first, which model of the frustrated packing (NSS or NEE) is present in the contact face and, (b) in case it is the NSS structure, which face of the (110) layer is actually in contact with the substrate. Indeed, the opposite faces of the layer have different structures: when seen from the north, the three helices expose one, two, and two methyl groups (a face hereafter described as 122) and when seen from the south, the helices expose two, one and one methyl groups (hereafter the 211 face) (cf. Figure 4a,b). We are therefore faced with a problem similar to but more complicated than that already encountered with epitaxially crystallized films of αiPP, for which two structurally different (010) contact faces are possible. As was the case in that study[23,24] the next step in the analysis of the epitaxy requires probing of the structure of the contact face in real space, i.e., resorting to AFM investigations.

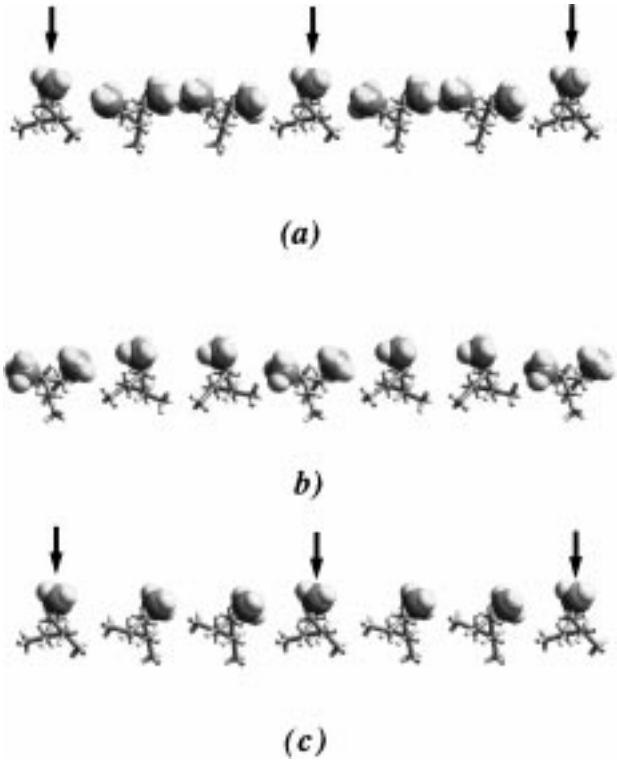

Figure 4. Profiles of the possible exposed faces of (110) planes of βiPP as seen along the *c* axis. Parts a and b show the opposite sides of the *same* (110) layer for a model of the type north south south (NSS); part c shows a layer of type north west west (NWW). Note in parts a and b a most unusual and characteristic consequence of the frustration, namely the fact that opposite sides of the (110) plane do not have the same topology. These faces are characterized by the number of methyl groups in each helix projecting in that face (shown as balls): 1,2,2 and 1,1,2. For commodity, a large unit cell has been created, corresponding to two $\approx$19 Å periodicities in the (110) plane. Note that the hand of the helices can in principle be determined when helices display *two* methyl groups, as in parts a and b.

2. Atomic Force Microscopy Investigation. In view of the ambiguity inherent to, and left by the above electron diffraction analysis, an AFM investigation of the (110) contact face of epitaxially crystallized βiPP appears warranted. The investigation has several objectives.

(a) The first is to establish the existence of a *19 Å periodicity* in the (110) contact face of βiPP. This periodicity corresponds to the distance between *three* helices, which should be visible if their azimuthal setting is not uniform: observation of this 19 Å periodicity would therefore correspond to a *"real space signature" of frustration.*

(b) The second is, as indicated above, to establish the exact structure of the contact face involved in the

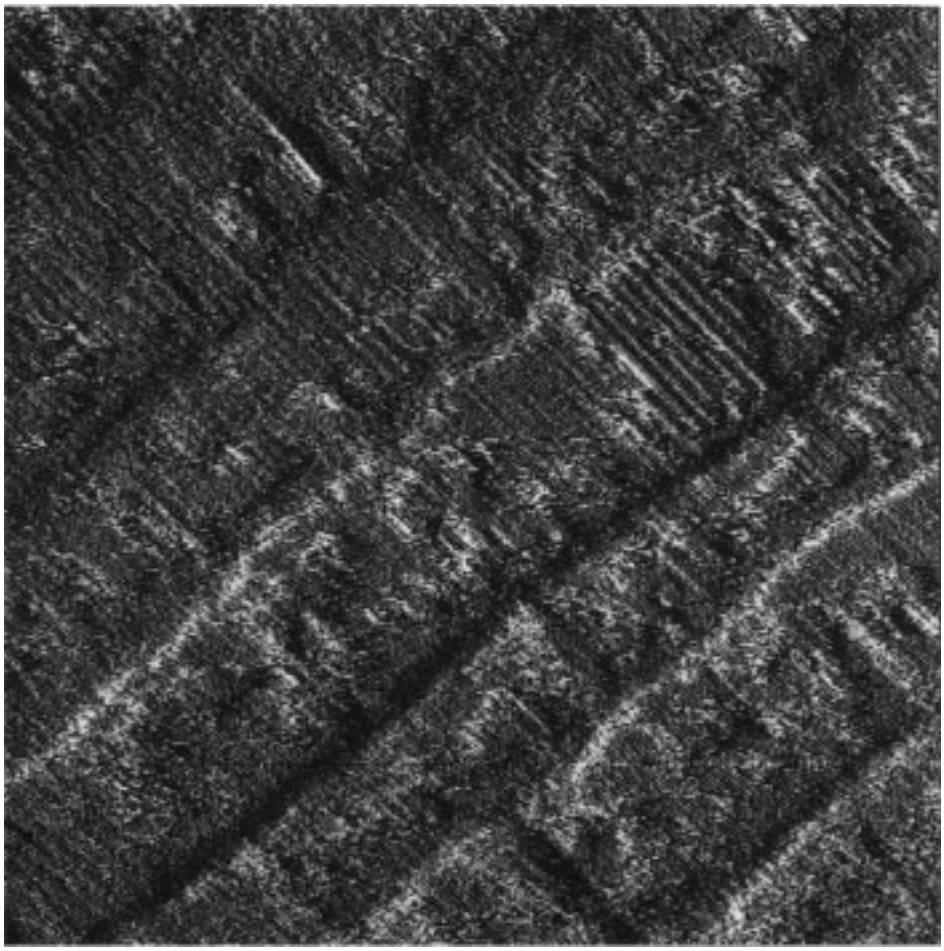

Figure 5. AFM picture of the contact face of βiPP in an area similar to that of Figure 2a. Chain axis orientation: from lower right to upper left (also best viewing conditions, at grazing incidence). Note the rows of methyl groups nearly parallel to the lamellar surface and the chain orientation which appears more prominently as striations normal to that lamellar surface in the center right part but also in most areas of the picture. Imaging conditions: in 2-propanol. Size of imaged area: 200×200 nm^2.

epitaxy, i.e. to distinguish between the two possible frustrated packing schemes (NSS or NEE) and, in case of NSS orientation, to discriminate between faces 122 and 211.

The above objectives rely on the unmatched *z*-axis resolution of the AFM technique. The different structures and faces should indeed have different "AFM signatures", as illustrated by their different profiles, which reflect the different azimuthal orientations of the chains. These are represented in Figure 4 (disregarding possible small variations of the azimuthal setting of any individual chain stem, which depends to some extent on the clinicity of the stem relative to its neighbors). On this basis, the NEE structure should be rather uncharacteristic and display three rows of "lone" methyl groups, with little difference in height: this structure would nearly approximate a "simple" one chain structure (Figure 4c). For NSS structures on the contrary, the 122 face is the most likely to display the three chains, with 19 Å periodicity. Indeed, the rows of "lone" methyl groups protrude above the plane of the "pairs" of methyl groups by an average of 1.5 Å. Similarly, the 211 face should display two rows of single methyl groups, alternating with a "deeper" helix exposing two methyl groups.

(c) A third objective of the AFM study might be considered: since, in the opposite faces of the NSS structure, either one or two helices expose two consecutive methyl groups of the chain, AFM should in principle be capable to visualize directly the *helical hand* of the helices in the contact plane, as has been done for syndiotactic polypropylene.[25] Note that this direct determination of helical hand was not possible for epitaxially crystallized αiPP since the chains in the contact plane expose only one methyl group (the helical hand was nevertheless deduced, indirectly, from the relative shifts of the helices in the (010) contact face).[23,24]

AFM investigations performed under liquid (in "wet" conditions) give consistently better results when high resolution is to be achieved.[24,25] Figure 5 represents a large scale image of the epitaxially crystallized βiPP. This picture is technically remarkable since it displays large scale features, namely the interdigitation and tapering of lamellae seen edge-on, while at the same time achieving methyl group resolution over the entire imaged area. Lamellar thicknesses are uneven, since they vary from about 30 to 50 nm. More importantly in the present context, the various chains building up the contact surface are clearly imaged as striations oriented from lower right to upper left of the picture, i.e., normal to the lamellar end surface orientation. The lateral periodicity of these striations is very prominent in some parts of the figure, in particular in the center right part. In this part, but more faintly also in many other areas of the picture, the lateral periodicity is 19 Å.

The local structure of the contact face is further illustrated in Figures 6a and 7a. In these views, the

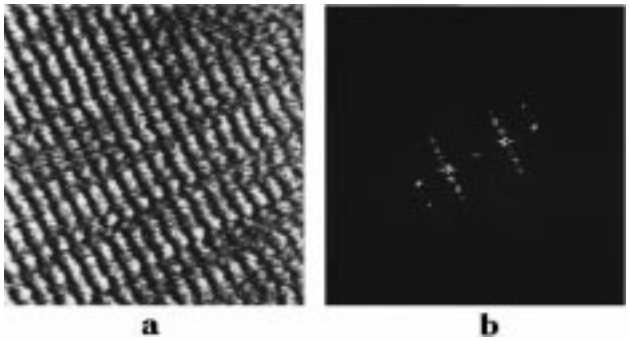

Figure 6. (a) High resolution, unfiltered AFM picture of the βiPP film as in Figure 2a. Chain axis orientation at ≈ 2 o'clock. Imaging conditions: in 2-propanol. Size of imaged area: 12.5 nm × 12.5 nm. (b) Two-dimensional fast Fourier transformed spectrum of the image in part a. Note the prominent organization in layers ≈6.5 Å apart, which corresponds to the iPP chain axis repeat distance, and the existence (mainly on the first layer line) of reflections indicating a lateral periodicity of ≈19 Å, which is a "signature" of the frustrated packing.

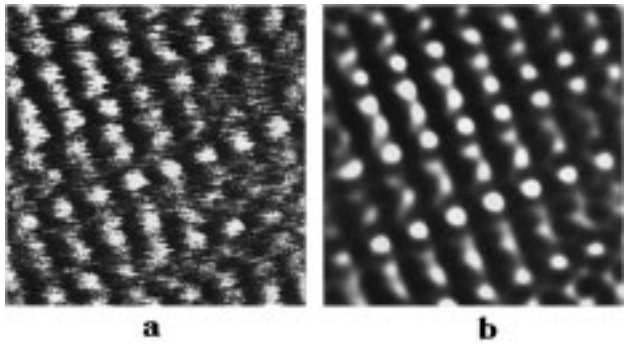

Figure 7. High-resolution AFM unfiltered **(a)** and Fourier-filtered **(b)** image of the contact face of epitaxially crystallized βiPP. Chain axis orientation: at 2 o'clock. Note, in the lower part of the pictures, the prominent rows of single methyl groups ≈19 Å apart, which suggest that the contact face is of type 122 (cf. Figure 4a). Size of imaged area: 5.5 nm × 5.5 nm.

periodicities along the chain axis direction (oriented at 2 o'clock) are more prominent, but striations parallel to the chain axis are also visible. The Fourier transform shown in Figure 6b is characterized by (a) layer lines 6.5 $Å^{-1}$ apart, corresponding to the c^* repeat distance of the 3-fold iPP helix (b) a lateral periodicity of 19 $Å^{-1}$ (and multiples thereof), which turns out to be better revealed on the first layer line than on the equator. These same periodicities appear also very prominently in the Fourier filtered picture of Figure 7b. This set of unfiltered, Fourier transform and filtered pictures therefore confirms that *AFM "sees" in real space the frustrated packing of* βiPP materialized by a 19 Å, three chains periodicity in the (110) plane.

It is possible to analyze further the pictures with limited risk of overinterpretation. We are in particular tempted to interpret the different surface patterns in terms of different frustrated structures. With reference to the above discussion (cf. Figure 4), the areas with prominent rows of methyl groups ≈6.5 Å apart (along the chain axis) and separated by the expected ≈19 Å suggest a packing scheme of the type NSS, which is most likely to display this periodicity, given the "hilliness" of the exposed (110) face. Further, the existence of a *single* row of methyl groups for the best resolved helix (cf. Figure 7a,b) suggests a contact face of type 122 (cf. Figure 4a). Other areas, such as the upper part of Figure 7 or the continuation of this same area in the upper part of Figure 6a (cf. also Figure 5), display a much fainter 19 Å periodicity, or even a shorter, one chain (6.35 Å) periodicity. We suggest that in these areas, the underlying structure is of the type NEE or NWW.

The present AFM data therefore indicate, or at least strongly suggest, that the contact face of the epitaxially crystallized βiPP films may correspond to different frustrated packings. The origin of this "surface polymorphism" cannot be determined at this stage. The NEE or NWW and NSS structures have small differences in packing energies. The substrate does not appear to favor one form exclusively, since the two structures coexist in the contact plane. Other factors must therefore be at play: most probably, the different local environments of up and down chains which either impose in the first place (i.e., on crystallization) one specific structure, or induce some surface reconstruction into the other form upon dissolution of the substrate. Such a reconstruction appears all the more likely that, upon dissolution, the surface helices which are probed by AFM are surrounded by four helices only instead of their usual six neighbors in the crystalline core.

The variations in surface organization of the (110) contact face do not seem to result from mechanical interactions with the AFM tip. This possibility must nevertheless be considered, since the different structures are interconvertible through only small rotations of some of the chains: for the NSS structure, it suffices that one chain out of the sequence of three be rotated on its axis by 60° to transform a 122 contact face into a 112 one. Azimuthal reorientations of 30° only would transform NEE into NSS structures and would be at the root of the above mentioned surface reconstructions. However, such mechanically induced transformations appear rather unlikely, given the weak tip−surface forces involved when working under liquid. As a matter of fact, they have *not* been observed when performing similar AFM experiments with the closely related αiPP phase: the contact faces exhibit a uniform pattern of methyl groups.[23,24] Also, images as shown in Figure 5 and 6a are obtained reproducibly for repeated scans, which implies that the surface is not harmed by the probing of the tip. This surface "strength" appears to be due to the fact that tip−helical stem contacts are local ones since they involve—ideally—only one methyl group of the stem, whereas the helical stem is embedded in and interacts with its crystallographic environment over its entire length, i.e., over ≈30−50nm.

Finally, it must be stressed that, for helices which expose two methyl groups, the latter have not been resolved—possibly because of the small scale (≈ 19 Å) "hilly" nature of the contact surface, in which the rows of "lone" methyl groups are projected ≈1.5 Å above the surrounding surface. As a consequence, it is not possible to "read" the helical hand of the helices, as was the case for syndiotactic polypropylene:[25] it is not therefore possible to determine the local "chirality" of the structure. The frustrated structure is chiral, and the iPP molecule, although chiral, is racemic: domains of both chiralities, separated by antiphase boundaries, should and must exist in βiPP.[2,9] When the resolution of the helix hand is reached, AFM will provide a direct means to observe the chirality in different lamellae and/or lamellar domains of the frustrated βiPP structure and therefore assess the size of antiphase domains, admit-

tedly under the rather special conditions of epitaxial crystallization.

3. Structural Requirements for βiPP Nucleating Agents. The current interest in βiPP nucleating agents arises from the fact that, as a result of its metastability and different spherulite architecture, the β phase has a lower melting temperature and improved mechanical properties (such as impact strength) than the more common α phase. Analysis of the structural relationships between the nucleators and βiPP helps establish, at least in their broad outlines, the structural requirements these nucleators must meet. We examine now these structural relationships and requirements in the broader context of epitaxy of helical polymers.

Two major classes of epitaxies of helical polymers have been observed so far. *In the first class*, the dimensional matching with the crystalline substrate takes place via the *interstrand distance*, which is indeed a prominent physical feature of the helices. Such epitaxies have been observed for α and γ iPP,[23] and isotactic poly(1-butene) in its form I.[26] The contact planes are made up of isochiral helices with 3_1 (or 3_2) symmetry with identical settings and constant relative *c* axis shifts: as a consequence, the side chains build up regular arrays or, more precisely, linear gratings. These gratings are involved in the epitaxy, since they match a substrate periodicity. As a result also, the matching is enantioselective, since the gratings of side chains, which follow roughly the helical path, are symmetrically oriented relative to the helix axis for right- and for left-handed helices: layers made of right- and of left-handed helices are, likewise, symmetrically oriented relative to the matching substrate periodicity.[21,23,26] *The second class* of epitaxies involves as a rule much less regular polymer contact faces. This structural irregularity may result from a nonrational helix geometry (as for the 11_3 helix of form II of poly(1-butene))[27] or from different settings when more regular helices are involved (4_1 helix of form III of poly(1-butene)).[27] In this second class, it is always the *chain axis repeat distance* which plays a major role in the dimensional match with the substrate.

The structure of the (110) contact face of βiPP, involved in the epitaxies on both γ-quinacridone and DCHT, is clearly of the second type: as a result of frustration, it combines different azimuthal settings and chain-axis shifts. The nearly perfect match between the iPP *helix axis repeat distance* (6.5 Å) and a similar substrate periodicity has been underlined when analyzing Figure 2c. The structural periodicity created by the end benzene rings aligned with a spacing of $c/2 = 6.7$ Å is evident from the molecular model of γ-quinacridone. The γ phase of quinacridone has a monoclinic unit cell with parameters $a = 13.78$ Å, $b = 3.90$ Å, $c = 13.40$ Å, and $\beta = 79.5°$. A representation of the *bc* contact plane involved in the epitaxy is shown in Figure 8. A similar structural analysis is not possible for DCHT since its crystal structure is not determined. However, the diffraction spots of the substrate on the first layer line of βiPP (cf. Figure 2c) suggest a similar match. Also, the similar chemical structures of γ-quinacridone and DCHT (linear, elongated molecules ended by benzyl or cyclohexyl rings) suggest that the contact face of DCHT is also an alignment of stacks of such rings.

A second favorable feature appears to be the *orthogonal geometry of the contact face*, which matches that of the (110) plane of βiPP: indeed, both γ-quinacridone and DCHT display diffraction spots which can be indexed on a rectangular lattice. The efficiency of DCHT in particular appears to result from an additional matching corresponding to reticular distances close to 9.5 Å: the major 19 Å periodicity in the (110) plane (*three* interhelix distances) correspond to *two* substrate periodicities. However, this analysis supposes a near orthorhombic unit cell for DCHT, since epitaxy rests on *surface* periodicities, and not on reticular distances of planes in diffracting position, normal to the surface.

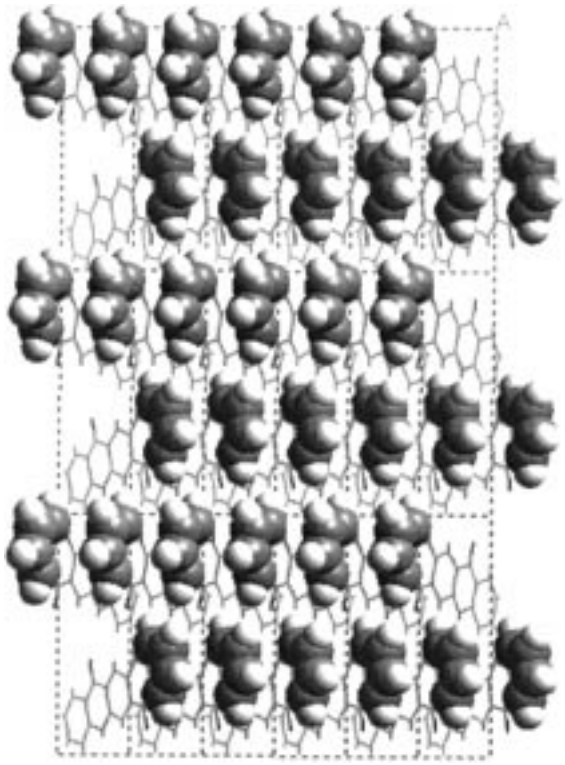

Figure 8. Surface structure of the contact face of γ-quinacridone involved in the epitaxy with βiPP (crystallographic data courtesy of Dr. Frank Leusen, Biosym-Molecular Simulations). Note the rectangular surface pattern and the rows of end benzene rings which generate a 6.7 Å grating matched by the 6.5 Å *c* axis repeat distance of βiPP.

A cautionary note is however in order: the 6.5 Å chain axis repeat distance of βiPP is not significantly different from the *interchain* distance in the (110) plane (6.35 Å) or, for that matter, the interchain distance in the (010) plane of αiPP (6.55 Å). Substrates suitable for the β phase may therefore act as α phase nucleating agents, but in that case the chains (and therefore lamellae) would be oriented at right angles to the "major" βiPP epitaxial relationship. We have indeed observed occasionally, in bright field electron micrographs of iPP crystallized on γ-quinacridone, very small patches of lamellae at right angles, but we could not determine, via electron diffraction, whether they are of β or αiPP. Finally, nucleating agents have other crystal faces with different lattice parameters and surface structure, which may well nucleate other crystal phases. Such a dual nucleating activity was indicated for γ-quinacridone by Rybnikar[28] ("E3B is also a very efficient nucleating agent for the α modification") and is suggested by the consistently lower β phase contents found for this nucleating agent (usually in the 70% range, as defined by the *k* factor[22]) compared to, for example, DCHT ($k > 95\%$).[14] Our preliminary observations suggest indeed that the end (010) surface of γ-quin-

acridone crystals is consistently decorated with αiPP quadrites (barely distinguishable in the thicker, erect parts of the polymer film in Figure 2b). This duality will be further investigated when γ-quinacridone crystals with better developed *ac* faces can be grown.

To conclude this section, it would appear that the main (and minimal) structural characteristics required for nucleating agents of β iPP are the existence in the contact faces of a 6.5 Å periodicity which matches the iPP chain axis repeat distance and an orthogonal cell geometry in that contact plane. Since these requirements are purely geometric (i.e. involve dimensional matchings only, but not the helix chirality), we are faced with a pleasant structural paradox: nucleating agents of the *chiral* βiPP crystal phase do *not* permit morphological recognition of the enantiomeric domains (*cf.* the single lamellar orientation, and symmetrical pattern of Figure 3b) whereas nucleating agents of the *racemic* αiPP, which interact more tightly with the helical paths of the first deposited layers, *permit* this discrimination through the different lamellar orientations.

Conclusion

Epitaxial crystallization of the metastable β polymorph of isotactic polypropylene has been achieved on single crystals of selected nucleating agents. Electron diffraction investigations indicate that the βiPP (110) plane is the contact plane. In the absence of the crystal structure of DCHT, the exact epitaxial relationship could not be worked out at the molecular level. A lattice matching between the *c* axis periodicity of iPP (6.5 Å) and a corresponding distance in the substrate crystal face appears as a prominent feature in the epitaxy: nucleating agents with this ≈ 6.5 Å periodicity and an orthogonal geometry of the contact face are likely to induce the βiPP polymorph. However, the similarity of the chain axis repeat distance and the interhelix packing in the (010) plane of the α phase may explain that some βiPP nucleating agents may also induce the α phase.[28]

AFM with methyl group resolution of the (110) contact plane reveals a lateral packing of helices with $a \approx 19$ Å periodicity, which results from different azimuthal settings of the chains and is a trademark of the frustrated packing of helices in βiPP. *The present AFM study therefore provides the first "real space" illustration of frustration in polymer crystallography*. Evidence suggests that different βiPP packing schemes exist in the contact plane, which have been defined as NEE or NWW, and NSS. For the latter, out of two possible profiles, that denoted 122 is the actual contact plane, with one "tip" and two "bases" of the three-fold helices exposed. Present limitations of resolution, possibly linked with the small scale "hilly" nature of the contact plane, do not allow direct observation of the helical hand, and therefore to assess the (co)existence of lamellae and/or lamellar domains with different helix chiralities, a possibility resulting from the crystallization of the chiral but racemic iPP in a chiral, frustrated β phase.

Acknowledgment. We wish to thank Dr. Frank Leusen (Biosym-Molecular Simulations, Waltham, MA and Cambridge, U.K.) for providing us with the atomic coordinates of the structure of γ-quinacridone prior to publication and Pr. Garbarczyk for kindly providing the thiazine derivative. The financial support of M.S. by Exxon Chemical International is gratefully acknowledged.

References and Notes

(1) Keith, H. D.; Padden, F. J., Jr.; Walter, N. M.; Wickoff, H. W. *J. Appl. Phys.* **1959**, *30*, 1485.
(2) Meille, S. V.; Ferro, D. R.; Brückner, S.; Lovinger, A. J.; Padden, F. J. *Macromolecules* **1994**, *27*, 2615.
(3) Lotz, B.; Kopp, S.; Dorset, D. *C. R. Acad. Sci. (Paris), Ser. IIb* **1994**, *319*, 187.
(4) Brückner, S.; Meille, S. V.; Petraccone, V.; Pirozzi, B. *Prog. Polym. Sci.* **1991**, *16*, 361.
(5) Lotz, B.; Wittmann, J. C.; Lovinger, A. *Polymer* **1996**, *37*, 4979.
(6) Toulouse, G. *Comm. Phys.* **1977**, *2*, 115.
(7) Puterman, M.; Kolpak, F. J.; Blackwell, J.; Lando, J. B. *J. Polym. Sci., Polym. Phys. Ed.* **1977**, *15*, 805.
(8) Cartier, L.; Spassky, N.; Lotz, B., *C. R. Acad. Sci. (Paris), Ser. IIb* **1996**, *322*, 429.
(9) Dorset, D. L.; McCourt, M. P.; Kopp, S.; Schumacher, M.; Okihara, T.; Lotz, B. *Polymer*, submitted for publication.
(10) Cartier, L.; Lotz, B. Manuscript in preparation.
(11) Cartier, L.; Lotz, B. Manuscript in preparation.
(12) Leugering, H. J. *Makromol. Chem.* **1967**, *109*, 204.
(13) Garbarczyk, J.; Paukszta, D. *Colloid Polym. Sci.* **1985**, *263*, 985.
(14) New Japan Chemical Co, Ltd, European Patent EP 93101000.3,; Japanese Patents JP 34088/92, JP 135892/92, JP 283689/92, JP 324807/92, 1992.
(15) Varga, J. In *Poly(propylene): Structure, blends and composites*; Vol. 1, Karger-Kocsis, J., Ed.; Chapman & Hall: London, **1995**, Vol. 1, Chapter 3, pp 56−115.
(16) Lotz, B.; Fillon, A.; Thierry, A.; Wittmann, J. C. *Polym. Bull.* **1991**, *25*, 101.
(17) Unpublished work from Dr. Frank Leusen, Biosym-Molecular Simulations, Inc. Private communication.
(18) Garbarczyk, J. *Acta Crystallogr.* **1985**, *C41*, 1062.
(19) Guanyi, S.; Hesheng, J.; Jingyun, Z.; Jing, H.; Shi, G.; Zhang, J., German Patent: P 36 10 644, 1986. Zhou, G.; He, Z.; Yu, J.; Han, Z.; Shi, G., *Makromol. Chem.* **1986**, *187*, 633. Tjong, S. C.; Shen, J. S.; Li, R. K. Y. *Polym. Eng. Sci.* **1996**, *36*, 100.
(20) PCD-Polymere Gesellschaft m.b. H. (Wolfschwenger, J.; and Bernreitner, K.); European Patent EP 682066 A1 951115, **1995**.
(21) Wittmann, J. C.; Lotz, B. *Prog. Polym. Sci.* **1990**, *15*, 909.
(22) Turner-Jones, A.; Aizlewood, J. M.; Beckett, D. R. *Makromol. Chem.* **1964**, *75*, 134.
(23) Stocker, W.; Magonov, S. N.; Cantow, H. J.; Wittmann, J. C.; Lotz, B. *Macromolecules* **1993**, *26*, 5915; Corrections: *Ibid.* **1994**, *27*, 6690.
(24) Stocker, W.; Graff, S.; Lang, J.; Wittmann, J. C.; Lotz, B. *Macromolecules* **1994**, *27*, 6677.
(25) Stocker, W.; Schumacher, M.; Graff, S.; Lang, J.; Wittmann, J. C.; Lovinger, A. J.; Lotz, B. *Macromolecules* **1994**, *27*, 6498.
(26) Kopp, S.; Wittmann, J. C.; Lotz, B. *Polymer* **1994**, *35*, 916.
(27) Kopp, S.; Wittmann, J. C.; Lotz, B., *Polymer* **1994**, *35*, 908.
(28) Rybnikar, F., *J. Macromol. Sci.—Phys.* **1991**, *B30*, 201.

MA971345D